

Polarised infrared and differential scanning calorimetry studies on oriented vinyl pipe materials

J. A. KWON, R. W. TRUSS

*Department of Mining, Minerals and Materials Engineering,
The University of Queensland, Brisbane, Qld 4072 Australia
E-mail: office@minmet.uq.edu.au*

The molecular orientation in a conventionally extruded PVC pipe, a uniaxially oriented PVC pipe and a biaxially oriented PVC pipe has been studied via Infrared dichroism. The degree of order or crystallinity has also been studied by Differential Scanning Calorimetry and also via Infrared Spectroscopy. The fundamental structural difference between the conventional and oriented pipes was that polymer chains were preferentially aligning in the hoop direction for oriented pipes whereas they were fairly isotropic in the conventional pipe with a slight preferential alignment in the axial direction. Analysis of the C–Cl stretching mode indicated that the uniaxially oriented pipe had much higher alignment of the C–Cl bond in the axial direction than the biaxial pipe, which correlates with higher fracture toughness for circumferential cracking in the biaxial pipe. Both DSC and Infrared spectroscopy detected little change in the crystallinity or order in the oriented pipes compared to the conventionally extruded pipes. © 2002 Kluwer Academic Publishers

1. Introduction

High-strength uPVC (HSPVC) or uniaxially oriented uPVC (OPVC) pipes were first developed by IMI Yorkshire Imperial Plastics (YIP) under the trade name “Superpolyorc” following the original work carried out by Imperial Chemical Industries [1]. Compared to the conventionally extruded uPVC pipe, the oriented pipes provide a number of advantages. These include production of pipes with reduced wall thicknesses for a given pressure rating, giving substantial material savings and greater hydrodynamic capacity by increasing the internal diameter of the pipe. More importantly, the mode of failure changes from cracks propagating radially through the wall of the pipe for the conventionally extruded pipes to cracks propagating circumferentially for the oriented pipes. Significant quantities of these pipes have been installed in Europe and Australia and field performance to date has been very good. Recently, an in-line process for making biaxial oriented pipes has been developed [2]. Despite the importance of these materials, little work has been published in quantifying the structure of the oriented pipes. This paper reports work using Infrared (IR) Spectroscopy and Differential Scanning Calorimetry (DSC) to characterise the structure of the PVC in a variety of oriented pipes. The fracture behaviour of these pipes has been reported elsewhere [3].

1.1. Infrared dichroism

PVC has been the subject of numerous Infrared Spectroscopy studies that have attempted to assign specific

molecular motions to regions of the spectrum [4–8]. IR dichroism uses plane polarized IR light to quantitatively measure the orientation of polymer molecules. By obtaining spectra with the plane of polarization rotated by 90° with respect to the specimen, a measure of the orientation in the specimen is obtained by changes in peak intensities. The orientation of the polymer can be described in terms of the dichroic ratio, which is the ratio of the IR absorbances in the perpendicular directions.

For each vibrational mode of a molecule, there is a transition moment vector, \mathbf{M} . The intensity of IR absorption depends on the angle (θ) that the electric vector of the incident radiation makes with \mathbf{M} [9]. Absorbance intensity (I) of plane polarized light is given by:

$$I = k(\mathbf{M} \cdot \mathbf{E})^2 = k(|\mathbf{M}| \cdot |\mathbf{E}|)^2 \cos^2 \theta \quad (1)$$

where k is a proportionality constant and \mathbf{E} is the electric vector. $|\mathbf{E}|$ is the magnitude of \mathbf{E} , $|\mathbf{M}|$ is the magnitude of \mathbf{M} and θ is the angle the \mathbf{E} makes with \mathbf{M} .

Thus, for $\theta = 90^\circ$, $I = 0$ will be observed and if $\theta = 0^\circ$, I will be a maximum. By defining the polarized electric vector directions while studying an oriented polymer, it is possible to calculate a dichroic ratio which will quantify the orientation.

1.2. Differential scanning calorimetry

A typical DSC thermogram of a rigid conventionally extruded PVC sample features a glass transition

temperature around 80°C and two broad peaks [10, 11]: endotherm *A*, with an enthalpy, $H(A)$, and endotherm *B*, with an enthalpy, $H(B)$. The point between these two endotherms has been termed the characteristic temperature (T_c) and it roughly represents the local temperature reached during processing the polymer.

Dawson *et al.* [12] attributed endotherm *A* to the remelting of crystallites which were melted during the processing operation and then recrystallised on cooling. Endotherm *B* was attributed mainly to the melting of crystallites which had not previously melted during the processing operation. Teh *et al.* [13] showed that the higher the processing temperature, the smaller the contribution from endotherm *B* and the higher the contribution from endotherm *A*. PVC is generally considered to contain a variety of crystalline species. The lamellar crystallites are the highest ordered structures in PVC, possessing the highest melting points (beyond 200°C). Fringed micelle and mesomorphous phases with lower order will have lower melting points. However, endotherms *A* and *B* cannot be distinguished to represent any of the crystallite types individually, since there is a spectrum of crystallite types leading to overlapping melting points.

2. Experimental

2.1. Materials

This work investigated three different types of vinyl pipe materials: conventionally extruded uPVC pipe, uniaxially OPVC pipe and biaxially OPVC pipe.

The uniaxially OPVC pipe was manufactured via a two stage process. In the first stage, a conventional uPVC pipe of approximately half the diameter and twice the wall thickness of the desired final OPVC pipe is extruded. In the second stage, this precursor pipe is expanded to the desired design diameter while holding the length of the pipe at a fixed distance (hoop orientation was $\sim 2:1$). Thus, a degree of biaxial orientation would be expected to be present in this pipe even though for the purposes of this work, it will be termed “uniaxial” oriented pipe. During the orientation stage, the precursor uPVC pipe is heated to above its glass transition temperature T_g (approx. 80°C), where it passes from a rigid state to a rubbery state. Deformation of the polymer in the rubbery state causes molecular orientation and which is “frozen-in” by cooling the material below its T_g . The optimum temperatures for generating orientation in uPVC lie between the T_g and approximately 120°C.

The biaxially OPVC pipe was made by an in-line manufacturing process [2] where after extrusion, a conventional pipe is expanded to the desired diameter while at the same time, the pipe is drawn in the axial direction. The hoop orientation was again 2:1 while the axial draw ratio was $\sim 20\%$. For the biaxial pipe, the precursor uPVC pipe is cooled down from approximately 190°C to the uPVC orientation temperature (between T_g and 120°C) via the thermal conditioning tank. The extrudate then passes through the expansion limit rollers and then into the spray cooling tank where high pressure water causes free expansion. Both oriented pipes

had nominal outside diameters of 160 mm and nominal wall thicknesses of 5 mm.

These oriented pipes were compared to a conventional extruded uPVC pipe with nominal outside diameter of 170 mm and wall thickness of 10 mm. Additionally, a uniaxially OPVC pipe end was studied. During orientation using the two-stage process, the pipe ends are heated with the rest of the pipe but are held fixed at constant diameter. Thus the pipe end has orientation levels going from conventionally extruded pipe, which is designated Level 1 to uniaxially OPVC pipe, designated Level 4. Level 2 and 3 corresponded to the intermediate levels of orientation as shown in Fig. 1. The pipe end had the advantage that different levels of orientation could be studied on the same pipe and that all of the samples from the pipe had experienced the same thermal history.

All pipes were supplied by Vinidex Tubemakers Pty Ltd. and were made from similar PVC resin formulations, which were Calcium/Zinc stabilised.

2.2. Infrared spectroscopy and dichroism

The definitions that will be used to refer to the pipe directions and planes are shown in Fig. 2. Specimens

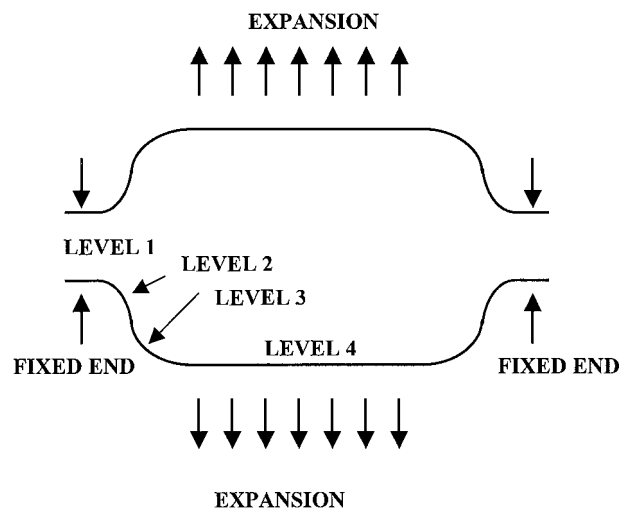


Figure 1 Designation of the different levels of orientation of the uniaxial pipe end. Levels 1, 2, 3, 4 represent increasing orientation from a conventionally extruded pipe, level 1, to a uniaxially oriented pipe, level 4.

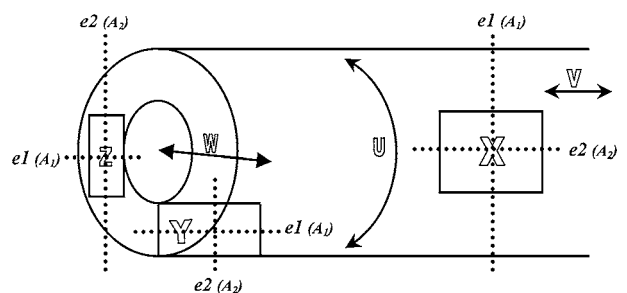


Figure 2 Definition of planes, directions and the polarised electric vectors e_1 and e_2 . X is the tangential plane, Y is the axial plane, Z is the cross-sectional plane, U is the hoop or circumferential direction, V is the axial, longitudinal or extrusion direction and W is the radial direction. A_1 and A_2 are the absorbance intensities measured with the electric vector polarized along e_1 and e_2 respectively for each of the three planes.

were microtomed from all pipes, in three planes, axial, tangential and cross-sectional planes, with the cutting direction parallel to e_2 for each plane. To evaluate the development of orientation in the uniaxial oriented pipe, specimens were microtomed from pipe ends in the tangential plane for all 4 levels of orientation, whereas only levels 1 and 4 were tested for the axial and cross-sectional planes. A microtome section was cut for one of the samples with the cutting direction perpendicular to the normal cutting direction, e_2 , and tested to ensure microtoming did not introduce orientation and affect the dichroic measurements.

A Reichert-Jung Ultracut machine was used for microtomy at room temperature, using a glass knife. Specimens were microtomed from the different planes (shown in Fig. 2) to be approximately 10 to 20 microns thick and were mounted on a holder over a 2 mm diameter hole. They were then tested using transmission Infrared Spectroscopy in a Perkin Elmer 2000 FTIR system equipped with an IR polarizer. To calculate dichroic ratios, there was a need to obtain spectra both parallel and perpendicular to the polarized electric vector. This was performed by physically rotating specimens by 90 degrees after each scan.

The directions of the polarized electric vectors were defined for each of the three planes as seen by the dotted lines in Fig. 2. A_1 and A_2 are the absorbance intensities measured with the electric vector polarized along e_1 and e_2 respectively. For each of the three planes, the dichroic ratio (D) was defined as:

$$D = A_2/A_1 \quad (2)$$

2.3. Differential scanning calorimetry

DSC specimens weighing approximately 5–10 mg were cut from different depths through the pipe wall and were placed in sealed pans to ensure that no HCl gas escaped during the test. DSC tests were conducted utilising a Perkin Elmer DSC7 system (equipped with a flue nitrogen gas stream) using a scan rate of 20°C/min. A scan of an empty tray was subtracted from each DSC curve to correct for the baseline. The system was calibrated using Indium during setup.

3. Results and discussion

A typical polarized IR spectrum for uniaxially oriented pipe is shown in Fig. 3. This spectrum shows

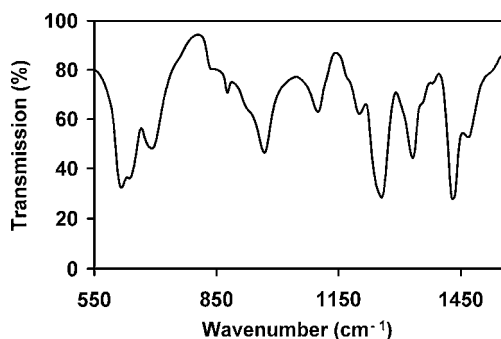


Figure 3 A typical polarised IR spectrum for uniaxially oriented pipe.

the typical absorbance bands found for PVC [4, 5]. The band region near 1100 cm^{-1} is usually assigned to a CC stretching mode while 1200–1300 cm^{-1} region bands are assigned to CH bending modes. CH_2 rocking modes are assigned to bands near 830, 960 and 970 cm^{-1} whereas bending, wagging and twisting modes are assigned to 1300–1450 cm^{-1} region bands. The 600–700 cm^{-1} region bands, due to C–Cl stretching vibrations were selected for determining preferential orientation of polymer chains in this study [4–6, 8, 14, 15]. A stretch mode of this type has a transition moment perpendicular to the backbone of the polymer molecule. For this arrangement, for $\theta = 90^\circ$, $I = 0$ whereas for $\theta = 0^\circ$, $I = \text{maximum}$. Using this band region and measuring the absorbance in orthogonal directions provided a convenient measure of the orientation of the PVC molecules in the pipes.

Fig. 4 shows the expanded 550 to 750 cm^{-1} band region of the spectra for the pipe end in the tangential, cross-sectional and axial planes. This Figure shows the difference in the absorbances at 615–616, 634–637 and 687–693 cm^{-1} after 90° rotation of the sample.

Fig. 5 shows the changes in the dichroic ratio for the three planes for samples from the uniaxially oriented pipe end. The pipe end samples had the advantage of displaying increasing uniaxial orientation from conventionally extruded pipe, level 1, through to the completed uniaxially oriented pipe, level 4. They had the added attraction of coming from the same pipe so that variations in formulation or processing thermal history of precursor pipes could be ignored. For level 1, the dichroic ratios were close to unity, which would be expected of an isotropic material. For the tangential plane, the dichroic ratio of level 1 was slightly less than unity. This suggested a slight preferred orientation of the molecules in the axial direction. Some small amount of orientation in the axial direction is not uncommon in conventionally extruded pipe. The dichroic ratio for the cross-sectional plane was also slightly less than unity. This would be consistent with a slight axial alignment of the molecules but with a slight preferred alignment of the C–Cl bonds in the radial direction. Alternatively, it could indicate a slight hoop orientation to the molecules in this plane. The dichroic ratio for the axial plane was not significantly different from unity indicating that the pipe was essentially isotropic on this plane. The other conventionally extruded pipe tested had a dichroic ratio for the axial plane slightly lower than the pipe end, which would be consistent with a slight radial orientation to the molecules. The overall picture then is one of the molecules having a slight spiral orientation down the axis of the pipe and a minor tilt of the molecules in the radial direction. It should be noted that the dichroism was never found to be strong in the conventionally extruded pipe suggesting that these pipes were close to isotropic. The effect of the uniaxial orientation process is best followed on the tangential plane. With increasing orientation of the pipe, level 2 to 4, the dichroic ratio for the tangential plane inverted from less than unity to greater than unity and increased with increasing orientation. Thus the molecular orientation has changed from a slight orientation in the axial direction to increasing

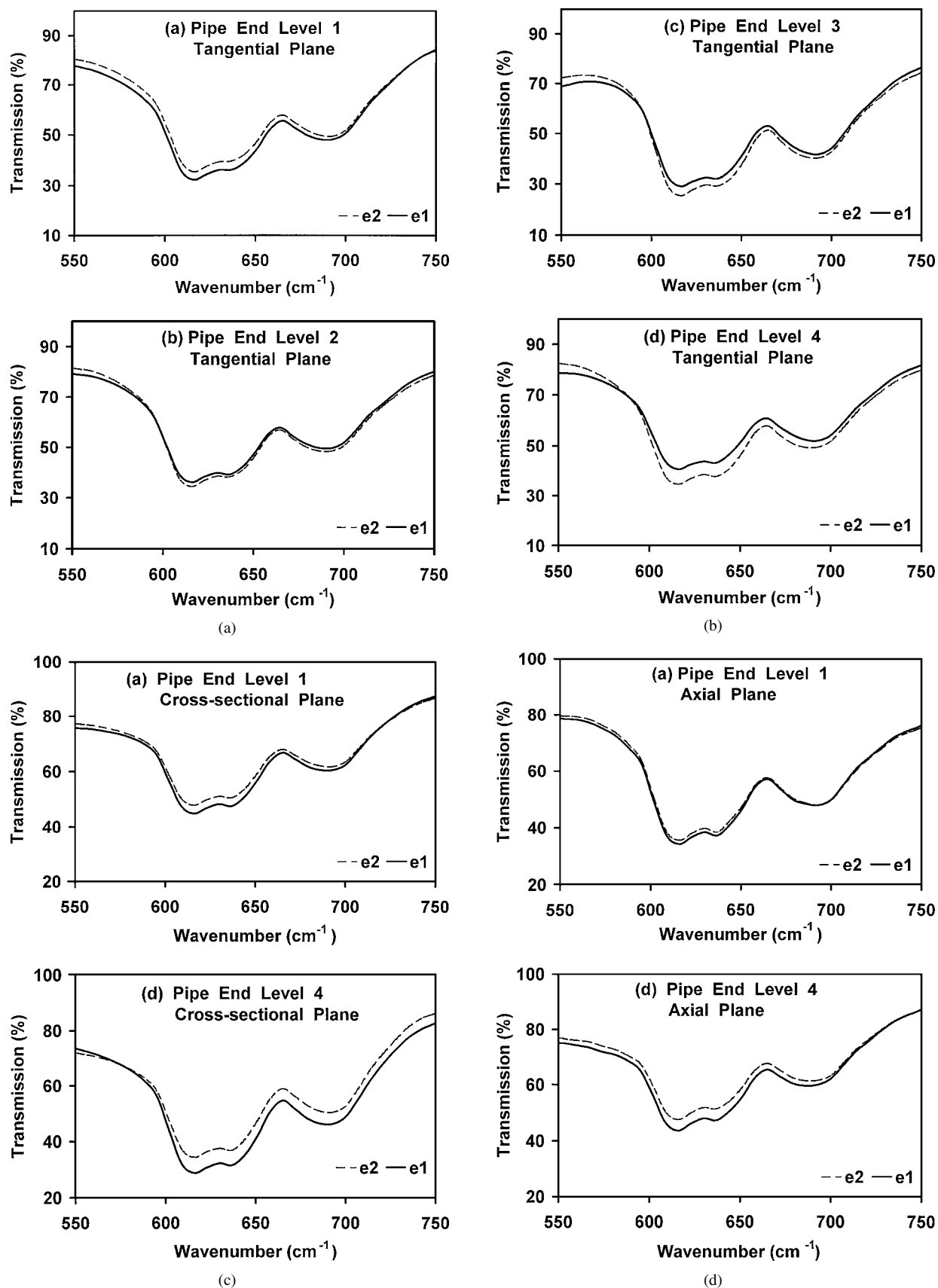


Figure 4 The 600–700 cm^{-1} region for the pipe end: tangential, cross-sectional and axial planes. (a) Level 1 (b) Level 2 (c) Level 3 (d) Level 4.

amounts of hoop orientation with pipe expansion. The dichroic ratios for the axial plane and the cross sectional plane were only measured for level 1 and level 4. In both cases, the ratios were less than 1 and decreased with orientation of the pipe. For level 4, a dichroic ratio of less than unity for the cross-sectional and axial

planes was consistent with molecular orientation in the hoop direction and the C–Cl bond in the axial direction.

Fig. 6 shows the dichroic ratio of the conventional, uniaxial and biaxial pipe in the three planes. The data for the conventional pipe and the uniaxially oriented pipe were consistent with the data for Level 1 and Level 4 of

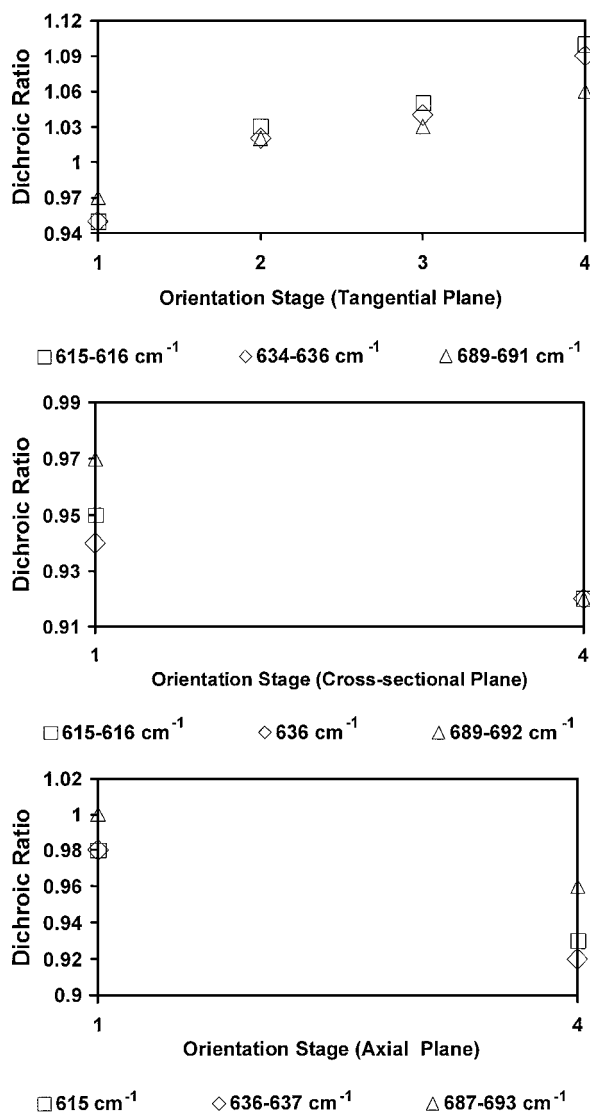


Figure 5 Dichroic ratios for the pipe end: tangential, cross-sectional and axial planes.

the pipe end respectively. The more significant result was that the IR dichroism in the tangential and axial planes was less in the biaxial pipe than in the uniaxial pipe. This might be expected since the extra axial draw in the biaxial pipe would induce some axial orientation in addition to the hoop orientation of the uniaxial pipe. A tilt of the molecules from the hoop direction in the axial direction would reduce A_2 in the tangential plane and A_1 in the axial plane. In the cross sectional plane, the dichroic ratio increased in the biaxial pipe compared to the uniaxial pipe. This implied that there were a larger number of C-Cl bonds aligned in the radial direction and fewer in the hoop direction for the biaxial pipe than the uniaxial pipe. This may suggest the possibility of stronger polar bonding in the radial direction between the molecules that may account for the higher delamination toughness measured for the biaxial pipe than the uniaxial pipe [3].

In many oriented polymer systems, the polymer orientation can be associated with an increase in the crystallinity. Commercial PVC has low crystallinity (<10%) but it is higher than that predicted from syndiotactic sequences known to exist in commercial PVC. Juijn [19, 25] and Windle and co-workers [18, 22, 23]

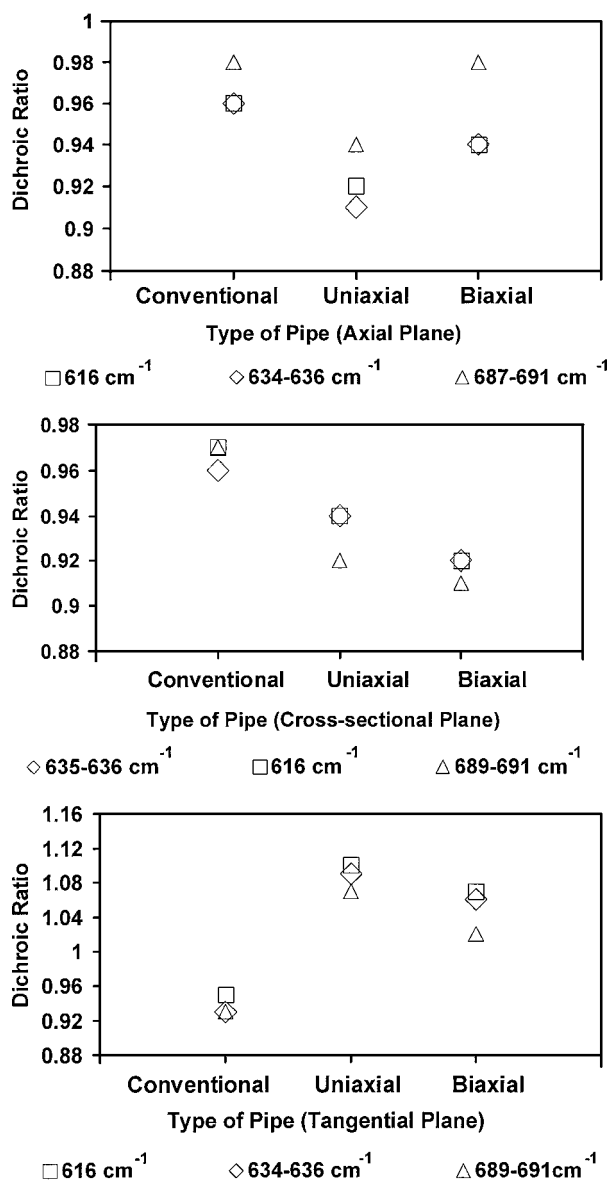


Figure 6 Dichroic ratios for the three pipes: tangential, cross-sectional and axial planes.

have shown that the PVC molecule can adopt a shape emulating conformation within chain sequences that allows greater measured crystallinity than would be expected from just the syndiotactic sequences in the chain. Orientation would alter the conformational state of the polymer chains and consequently, thermal analysis and examination of the crystalline absorptions in the IR data were conducted to assess changes in the crystalline order in the oriented pipes.

The DSC thermograms for conventional, uniaxial and biaxial pipes are shown in Fig. 7 at different points through the wall depth. The main features of the thermograms for the oriented pipes were similar to those of the conventional pipe. All of the pipes showed a glass transition at $\sim 80^\circ\text{C}$, followed by two melting endotherms between approximately 110 to 220°C . There is an indication of a feature on the curve for the uniaxial pipe that could be due to the orientation temperature at around 95°C . However, it was somewhat ambiguous, since it lay between and was superimposed on the post T_g enthalpy peak and the enthalpy peak due to the melting of a processing additive.

TABLE I Thermal analysis data for all three pipe types tested

Pipe	Position	$H(A)$ (J/g)	$H(B)$ (J/g)	$H(A) + H(B)$ (J/g)	T_g (°C)	T_c (°C)
Conventional	1-Outer wall (i)	11.7	0.3	12	82	203
	2 (j)	2.6	2.5	5.1	82	178
	3 (k)	1.7	2.8	4.5	81	172
	4 (l)	1.9	2.9	4.8	82	174
	5-Inner wall (m)	2.0	1.7	3.7	82	177
Uniaxial	1-Outer wall (i)	3.8	0.9	4.7	84	184
	2 (j)	2.7	1.5	4.2	85	175
	3 (k)	1.4	1.9	3.3	85	174
	4 (l)	2.1	1.2	3.3	85	183
	5-Inner wall (m)	3.6	0.7	4.3	84	187
Biaxial	1-Outer wall (i)	5.9	0.3	6.2	83	200
	2 (j)	3.3	2.0	5.3	81	183
	3 (k)	3.8	2.7	6.5	82	178
	4 (l)	4.2	2.2	6.4	83	180
	5-Inner wall (m)	4.2	1.8	6.0	82	179

The key enthalpies and temperatures were determined and are listed in Table I. The average T_g for the uniaxial pipe, 85°C, was a few degrees higher than that of the conventional and biaxially oriented pipes at 82°C. If it is assumed that all positions through the wall of the pipe experienced the same cooling rate, then a standard deviation can be determined of ~0.5°C for the conventional and the uniaxial oriented pipe and ~0.8°C for the biaxial pipe. These values are probably an overestimate of the standard deviation as the assumption of similar cooling rates through the wall of the pipe is incorrect. However, the standard deviations do suggest that the measured difference in T_g was significant. This difference, although small, is probably a result of the slower cooling rate through the glass transition in the uniaxial oriented pipe.

The high value of $H(A)$ for the outer wall of the conventional pipe (11.7 J/g) is consistent with previous DSC studies on PVC. Gilbert and Vyvoda [10] found a rapid increase in $H(A)$ with processing temperature for processing temperatures >~200°C in compression moulded PVC and for PVC melt mixed in a Brabender. They obtained values of $H(A)$ of 5–11.5 J/g with stock temperatures between 200–225°C, which is consistent with the values for the outer wall of the extruded pipe here. At high values of T_c , $H(B)$ tends to be small so high values of $H(A)$ imply high values of the total crystallinity. Conditions of high T_c , however, only apply near the outside wall of the pipe.

Ignoring this high value at the outside wall of the pipe, the biaxial pipe showed a slightly higher overall crystallinity given by $H(A) + H(B)$ than the uniaxial and conventional pipes. The combined melting enthalpy for the biaxial pipe was 6.1 J/g while for the uniaxial pipe the value was 3.8 J/g and for the conventional pipe it was 4.5 J/g. The standard deviation for these results was estimated as ~0.6 J/gm. The higher total crystallinity of the biaxial pipe was largely due to a higher $H(A)$ for this pipe. The reason for this is uncertain but it may be due to the fact that the biaxial pipe was made via an in-line process where the original extruded pipe was not quenched to room temperature in a water bath but cooled to the orientation temperature in a thermal conditioning tank. Hence, it may have

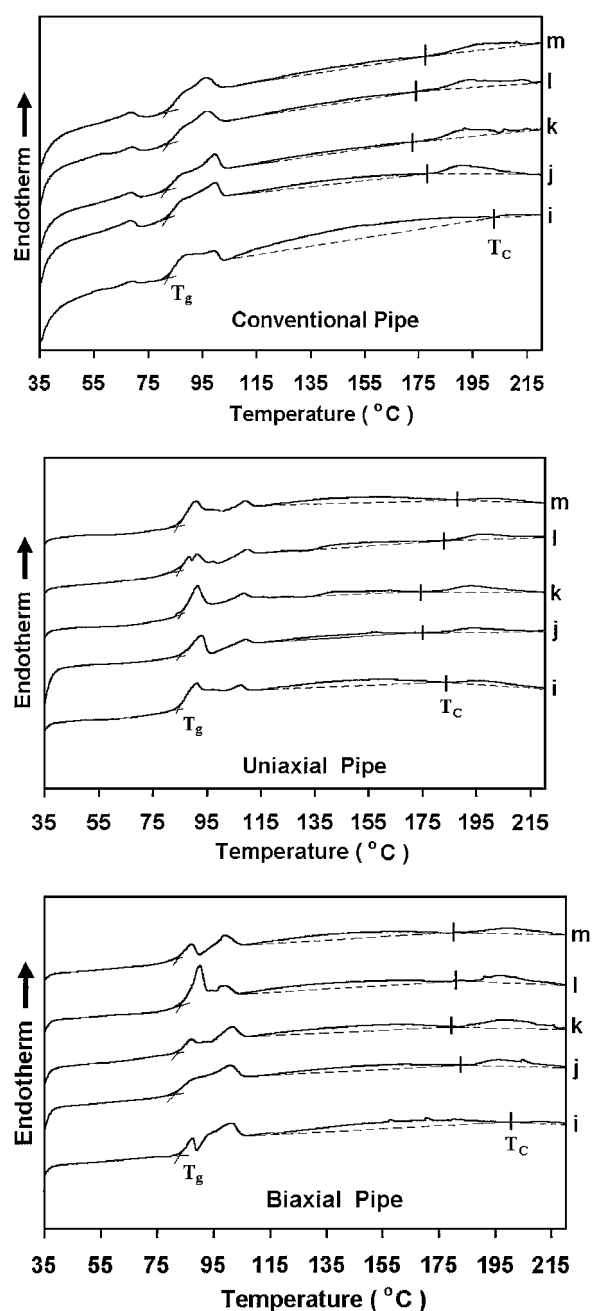


Figure 7 DSC thermograms for the three pipes through the wall depth. i: outer wall; m: inner wall; j, k, l: intermediate wall depths.

experienced a longer time at temperatures where order could have formed than the conventional or uniaxial pipes.

The distribution of the measured T_C through the wall thickness did not appear to be affected by the orientation process. The measured value of T_C was lowest in the middle of the wall and increased approaching the inner and outer wall surfaces for the conventional pipe. Although these measurements were not repeated a sufficient number of times to determine a standard deviation, the results are consistent with other reported data for conventional pipe by Choi *et al.* [11] and Clark [16].

A number of researchers have used Infrared Spectroscopy to also quantify the order in PVC. It is generally agreed that the 601–605 cm^{-1} region bands arise from C–Cl stretching in the crystalline regions and the 612–615 cm^{-1} and 685–693 cm^{-1} region bands arise from amorphous regions [4–6, 8, 14, 17]. For all the IR spectra that were measured for all of the pipe samples, the C–Cl stretching bands at 601–604 cm^{-1} , which have been assigned to motions from crystalline regions, were not observed. This could mean either that the crystalline regions were not present in the manufactured pipe or that their contribution was so small that it was swamped by the interference from overlapping peaks coming from the amorphous polymer. In either case, it indicated that crystallinity was not well developed in any of the pipes.

Commercial PVC is known to possess only a small degree of syndiotacticity. Yet, the crystallinity in low syndiotactic PVC has been reported to be approx. 5–10% [20]. Juijn [19, 25], Hobson and Windle [18] and Flores and Windle [22, 23] have addressed this seeming paradox.

Juijn [19, 25] calculated the maximum amount of crystallinity possible in atactic PVC as a function of minimum sequence length. The maximum amount of crystallinity would be 0.45% for syndiotactic sequences of 12 repeating units. Using WAXD, Lemstra *et al.* [24] estimated the coherence diffraction length along the chain direction to be 14 repeating units. For syndiotactic sequences 13 repeating units or more, the maximum amount of crystallinity possible would be 0.27%.

Juijn [19, 25] was the first to suggest that some isotactic units must be included in the otherwise syndiotactic PVC crystallites in order to account for the relatively high percentage of crystallinity found in commercial atactic PVC. Hobson and Windle [18] confirmed this to be possible by using molecular modeling. They found an isotactic conformation with a subsidiary energy minimum which enables the isotactic sequences to emulate the general shape (approximate Van der Waals envelope) and axial repeat of syndiotactic sequences in the planar zigzag conformation of minimum energy. The general shape of isotactic sequences will emulate that of syndiotactic sequences if every alternate backbone torsion angle is rotated one way and then the other by approximately 30 degrees away from the planar zigzag setting.

Isotactic segments forced into planar zigzag conformation can act as crystal ‘defects’ [26]. The packing of

TABLE II IR indexes for all three pipes. Based on the absorbance intensities measured with the electric vector polarized along e_1 and e_2 respectively for each of the three planes

Plane	Pipe	e_2 $D_{634-637}/$ $D_{615-616}$ Index	e_1 $D_{634-637}/$ $D_{615-616}$ Index
Tangential	Conventional	0.93	0.95
	Uniaxial	0.95	0.96
	Biaxial	0.94	0.95
Axial	Conventional	0.95	0.96
	Uniaxial	0.92	0.93
	Biaxial	0.93	0.94
Cross-sectional	Conventional	0.96	0.96
	Uniaxial	0.96	0.95
	Biaxial	0.96	0.97

a mixed tacticity molecule with an odd number of isotactic ‘defects’ causes a high disturbance in the crystal due to the shift by one unit of the full structural repeat. Chlorines in the mixed tacticity chain will face the chlorines of the nearest syndiotactic molecules. As a result, the packing energy of the system increases. On the other hand, a mixed tacticity molecule with an even number of isotactic units can be accommodated within a syndiotactic crystal environment when the isotactic units adopt the ‘shape-emulating’ conformation, providing the means for co-crystallization [22, 23].

There are conflicting views in the literature regarding the assignment of the 627–638 cm^{-1} region absorption bands. In some cases, they are assigned to the crystalline [5, 14] phase in the polymer and in others to an amorphous phase [4, 8, 17]. Krimm and Liang [6] stated that the 635 cm^{-1} perhaps arises either from interactions in the crystalline regions of the polymer or from rotational isomers of the polymer chain, which are present in the amorphous regions. The inconsistency in the assignment of the 627–638 cm^{-1} region bands may be due to syndiotactic chain ‘shape emulation’ [18]. It would have been difficult to assign the 627–638 cm^{-1} region bands without looking for this ‘shape emulating’ conformation. Such an assignment is consistent with the work of Krimm and Enomoto [14] who assigned the 627–638 cm^{-1} region bands to ‘less favourable’ conformations associated with isotactic sequences. If this assignment is correct, the index $D_{627-638}/D_{612-615}$ would represent the relative proportion of ‘shape emulating’ conformations in chain sequences.

Table II lists ratios of absorbance intensities of 634–637 cm^{-1} to 615–616 cm^{-1} region bands that were observed for the pipes. For both e_1 and e_2 , there appears to be very little difference in the value of the $D_{634-637}/D_{615-616}$ index for all the pipes (within 0.95 ± 0.02). If the above assignment is correct then it implies that the relative proportion of ‘less favourable’ conformations did not change during the pipe orientation process. A similar result was obtained for the uniaxially oriented pipe end.

4. Conclusions

Infrared Dichroism was used to determine the molecular orientation of a conventionally extruded pipe, a

uniaxially oriented pipe and a biaxially oriented pipe. The conventional pipes had little orientation. A dichroic ratio of less than one for the tangential plane indicated a small preferred orientation in the axial direction. Results for the cross-sectional and axial planes suggested slight tilting of the chains in the hoop and radial directions. Both oriented pipes displayed distinct molecular orientation in the hoop direction and this was higher in the uniaxial pipe than the biaxial pipe. In the uniaxial pipe, the C—Cl bonds showed a preferred orientation in the axial direction while these bonds had a higher radial orientation in the biaxial pipe.

The IR results indicate little difference in the order within the PVC between the conventional pipe and the two oriented pipes. The DSC results also indicate little difference in the order within the PVC between the conventional and uniaxial pipes but does indicate a slightly higher level of crystallinity in the biaxial pipe compared to the other two pipes. This can be attributed to the different thermal history of the biaxial pipe. It should be noted that the orientation in the pipes was relatively modest and probably insufficient for new crystalline oriented structures to form.

Acknowledgments

This work was completed with the aid of an Australian Research Council SPIRT grant and collaboration and financial support from Australian Vinyls Corporation and Vinidex Tubemakers Pty. Ltd. In particular, our gratitude goes to Peter Chapman (Vinidex), Dr. Brian Casey (AVC) and Lucy Croker (Vinidex).

References

1. R. C. STEPHENSON, *J. Vinyl Tech.* **5**(1) (1983) 13.
2. P. G. CHAPMAN and L. ÅGREN, "A new technology for in-line manufacture of biaxially oriented PVC Pipes" (Plastics Pipes X, Gothenburg, Sweden, 1998).

3. J. A. KWON and R. W. TRUSS, *Eng. Fract. Mech.*, in press.
4. M. TASUMI and T. SHIMANOCHI, *Spectrochimica Acta* **17** (1961) 731.
5. S. KRIMM, V. L. FOLT, J. J. SHIPMAN and A. R. BERENS, *J. Polym. Sci. A* **1** (1963) 2621.
6. S. KRIMM and C. Y. LIANG, *J. Polym. Sci.* **XXII** (1956) 95.
7. P. COUSIN, *J. Vinyl Tech.* **10** (1988) 175.
8. M. THEODOROU and B. JASSE, *J. Polym. Sci.: Polym. Phys. Ed.* **21** (1983) 2263.
9. J. L. KOENIG, "Spectroscopy of Polymers" (American Chemical Society, 1992).
10. M. GILBERT and J. C. VYVODA, *Polymer* **22** (1981) 1134.
11. P. CHOI, M. LYNCH, A. RUDIN, J. W. TEH and J. BATISTE, *J. Vinyl Tech.* **14** (1992) 156.
12. P. C. DAWSON, M. GILBERT and W. F. MADDAMS, *J. Polym. Sci.: Pt. B: Polym. Phys. Ed.* **29** (1991) 1407.
13. J. W. TEH, A. A. COOPER, A. RUDIN and J. L. H. BATISTE, *J. Vinyl Tech.* **11** (1989) 33.
14. S. KRIMM and S. ENOMOTO, *J. Polym. Sci. A* **2** (1964) 669.
15. S. A. JABARIN, *Polym. Eng. Sci.* **31** (1991) 638.
16. D. J. M. CLARK, Ph.D. thesis, University of Queensland, Australia, 1995.
17. R. BIAIS, C. GENY, C. MORDINI and M. CARREGA, *Br. Polym. J.* (1980) 179.
18. R. J. HOBSON and A. H. WINDLE, *Polymer* **34** (1993) 3582.
19. J. A. JUIJN, G. H. GISOLF and W. A. DE JONG, *Kolloid Z. Z. Polym.* **251** (1973) 465.
20. R. J. D'AMATO and S. STRELLA, *Appl. Polym. Symp.* **8** (1969) 275.
21. Q. T. PHAM, J. MILLAN and E. L. MADRUGA, *Makromol. Chem.* **175** (1974) 945.
22. A. FLORES and A. H. WINDLE, in Physical Aspects of Polymer Science, 17th Biennial Meeting, University of Leeds, 1995.
23. *Idem.*, *Comp. Theor. Polym. Sci.* **6** (1996) 67.
24. P. J. LEMSTRA, A. KELLER and M. CUDBY, *J. Polym. Sci.: Polym. Phys. Ed.* **16** (1978) 1507.
25. J. A. JUIJN, Ph.D. thesis, Technical University Delft, 1972.
26. A. MICHEL and A. GUYOT, *J. Polym. Sci. C* **33** (1971) 75.

Received 6 November 2000
and accepted 31 December 2001